$K^+\Lambda$ photoproduction in a dynamical coupled-channel approach

Deborah Rönchen
HISKP, Bonn University

In collaboration with M. Döring, U.-G. Meißner, J. Haidenbauer, H. Haberzettl, K. Nakayama

PWA10/ATHOS5
July 2018, Beijing, China

Supported by DFG, NSFC
HPC support by Jülich Supercomputing Centre

Introduction: Baryon spectrum in experiment and theory

- **Theoretical** predictions: lattice calculations and quark models

Lattice calculation (single hadron approximation):

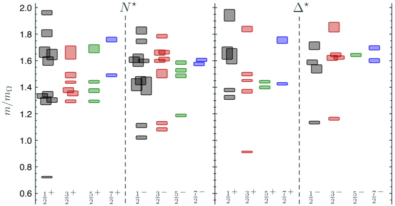

[Edwards *et al.*, Phys.Rev. D84 (2011)]

- above 1.8 GeV much more states are predicted than observed,

  "Missing resonance problem"

- PDG listing: Until recently major part of the information from πN elastic

- **Experimental** studies: Photoproduction: e.g. from JLab, ELSA, MAMI, GRAAL, SPring-8

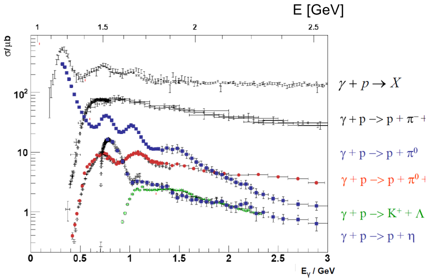

source: ELSA; data: ELSA, JLab, MAMI

- enlarged data base with high quality for different final states
- (double) polarization observables
  $\rightarrow$ alternative source of information besides $\pi N \rightarrow X$, e.g. $\gamma p \rightarrow K\Lambda$

Introduction: Baryon spectrum in experiment and theory

- **Theoretical** predictions: lattice calculations and quark models

  Relativistic quark model:

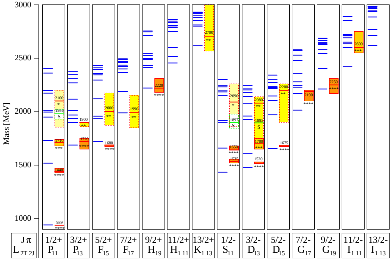

Löring *et al.* EPJ A 10, 395 (2001), experimental spectrum: PDG 2000

- above 1.8 GeV much more states are predicted than observed,

  "Missing resonance problem"

- PDG listing: Until recently major part of the information from πN elastic

- **Experimental** studies:
  Photoproduction: e.g. from JLab, ELSA, MAMI, GRAAL, SPring-8

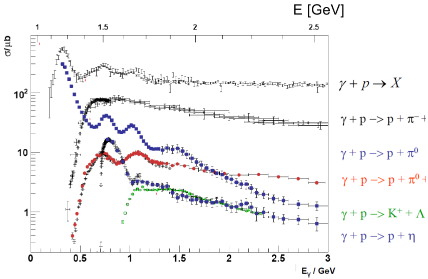

source: ELSA; data: ELSA, JLab, MAMI

- enlarged data base with high quality for different final states

- (double) polarization observables
  $\rightarrow$ alternative source of information besides $\pi N \rightarrow X$, e.g. $\gamma p \rightarrow K \Lambda$

Kaon photoproduction

KY final states

- certain (missing) resonances might couple predominantly to strangeness channels
- measurement of recoil polarization easier due to self-analyzing weak decay of hyperons
  $\rightarrow$ more recoil and beam-recoil data, which are needed for a complete experiment

- Photoproduction of pseudoscalar mesons:

  $\Rightarrow$ 16 polarization observables:

  asymmetries composed of **beam**, **target** and **recoil** polarization measurements

  $\Rightarrow$ **Complete Experiment**: unambiguous determination of the amplitude

  8 carefully selected observables Chiang and Tabakin, PRC 55, 2054 (1997)

  e.g. $\{\sigma, \Sigma, T, P, E, G, C_x, C_z\}$

  (unambiguous up to an overall phase and experimental uncertainties)

Different analyses frameworks: a few examples

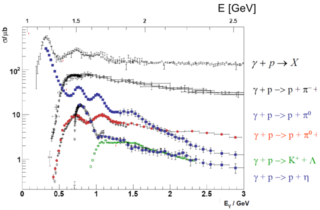

$\Longleftrightarrow$

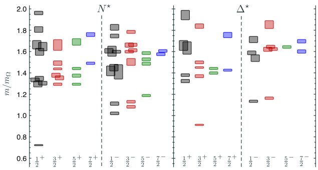

[Edwards *et al.*, Phys.Rev. D84 (2011)]

- GWU/SAID approach: PWA based on Chew-Mandelstam K-matrix parameterization
- unitary isobar models: unitary amplitudes + Breit-Wigner resonances
  MAID, Yerevan/JLab, KSU
- multi-channel K-matrix: BnGa (mostly phenomenological Bgd, N/D approach), Gießen (microscopic Bgd)
- dynamical coupled-channel (DCC): 3-dim scattering eq., off-shell intermediate states
  ANL-Osaka (EBAC), Dubna-Mainz-Taipeh, Jülich-Bonn

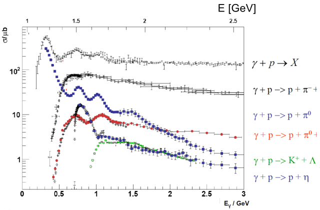

$\Longleftrightarrow$

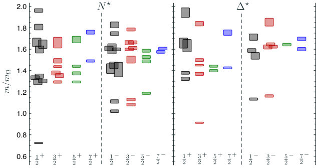

[Edwards *et al.*, Phys.Rev. D84 (2011)]

- GWU/SAID approach: PWA based on Chew-Mandelstam K-matrix parameterization
- unitary isobar models: unitary amplitudes + Breit-Wigner resonances
  MAID, Yerevan/JLab, KSU
- multi-channel K-matrix: BnGa (mostly phenomenological Bgd, N/D approach),
  Gießen (microscopic Bgd)
- dynamical coupled-channel (DCC): 3-dim scattering eq., off-shell intermediate states
  ANL-Osaka (EBAC), Dubna-Mainz-Taipeh, Jülich-Bonn

The Jülich-Bonn DCC approach

Dynamical coupled-channels (DCC): **simultaneous** analysis of different reactions

The scattering equation in partial-wave basis

$$\langle L'S'p'|T^{IJ}_{\mu\nu}|LSp\rangle = \langle L'S'p'|V^{IJ}_{\mu\nu}|LSp\rangle + \sum_{\gamma,L''S''}\int_0^\infty dq \quad q^2 \quad \langle L'S'p'|V^{IJ}_{\mu\gamma}|L''S''q\rangle \frac{1}{E - E_\gamma(q) + i\epsilon} \langle L''S''q|T^{IJ}_{\gamma\nu}|LSp\rangle$$

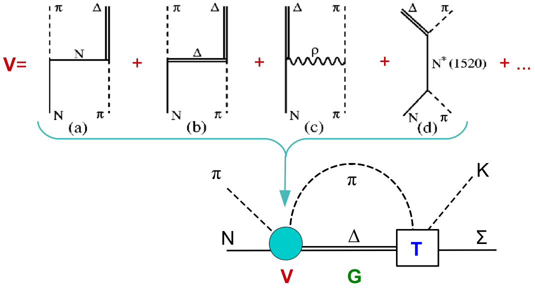

- potentials V constructed from effective $\mathcal{L}$
- s-channel diagrams: T^P
  genuine resonance states
- t- and u-channel: T^{NP}
  dynamical generation of poles
  partial waves strongly correlated
- contact terms

The Jülich-Bonn DCC approach

Resonance states: **Poles in the T-matrix** on the 2^{nd} Riemann sheet

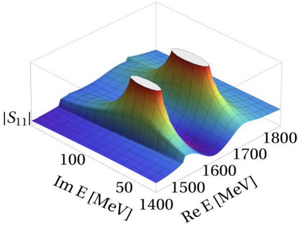

Re(E_0) = "mass", -2Im(E_0) = "width"

- pole position E_0 is the same in all channels
- residues→ branching ratios

- (2-body) unitarity and analyticity respected
- 3-body $\pi\pi N$ channel:
  - parameterized effectively as $\pi\Delta$, σN, ρN
  - $\pi N/\pi\pi$ subsystems fit the respective phase shifts

  ↳ branch points move into complex plane

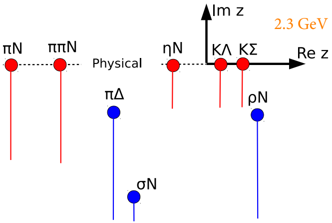

Multipole amplitude

$$M^{IJ}_{\mu\gamma} = V^{IJ}_{\mu\gamma} + \sum_{\kappa} T^{IJ}_{\mu\kappa} G_{\kappa} V^{IJ}_{\kappa\gamma}$$

(partial wave basis)

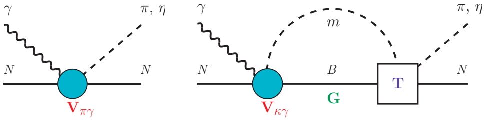

$m = \pi, \eta, K$, $B = N, \Delta, \Lambda$

$T_{\mu\kappa}$: Jülich hadronic T-matrix → Watson's theorem fulfilled by construction
→ **analyticity of T**: extraction of resonance parameters

Photoproduction potential: approximated by energy-dependent polynomials

$\mathbf{V}_{\mu\gamma}(E,q) =$ 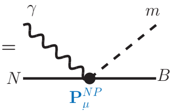 $+$ 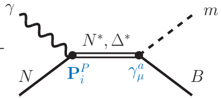 $= \dfrac{\tilde{\gamma}^a_{\mu}(q)}{m_N} P^{\mathrm{NP}}_{\mu}(E) + \sum_i \dfrac{\gamma^a_{\mu;i}(q) P^{\mathrm{P}}_i(E)}{E - m^b_i}$

$\tilde{\gamma}^a_{\mu}$, $\gamma^a_{\mu;i}$: hadronic vertices → correct threshold behaviour, cancellation of singularity at $E = m^b_i$
→ $\gamma^a_{\mu;i}$ affects pion- and photon-induced production of final state mB

i: resonance number per multipole; μ: channels πN, ηN, $\pi\Delta$, KY

Data analysis and fit results

Fit parameters:

s-channel: resonances (T^P)

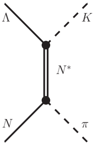

m_{bare} + f_{mBN^*}

- $\pi N \to \pi N$
  $\pi^- p \to \eta n,\ K^0\Lambda,\ K^0\Sigma^0,\ K^+\Sigma^-$
  $\pi^+ p \to K^+\Sigma^+$

$\Rightarrow$ 134 free parameters
  11 N^* resonances $\times$ (1 m_{bare}+ couplings to πN, ρN, ηN, $\pi\Delta$, $K\Lambda$, $K\Sigma$)
  + 10 Δ resonances $\times$ (1 m_{bare}+ couplings to πN, ρN, $\pi\Delta$, $K\Sigma$)

- contact terms: one per partial wave, couplings to πN, ηN, ($\pi\Delta$,) $K\Lambda$, $K\Sigma$
  $\Rightarrow$ 61 free parameters

- $\gamma p \to \pi^0 p$, $\pi^+ n$, ηp, $K^+\Lambda$:
  couplings of the polynomials
  $\Rightarrow$ 566 free parameters

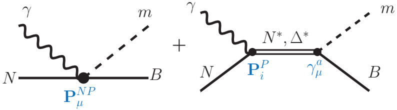

$\Rightarrow$ 761 in total, calculations on the JURECA supercomputer [Jülich Supercomputing Centre, *JURECA: General-purpose supercomputer at Jülich Supercomputing Centre*, Journal of large-scale research facilities, 2, A**62** (2016)]

- t- & u-channel parameters: fixed to values of hadronic DCC analysis (JüBo 2013)

Reaction	Observables (# data points)	p./channel
$\pi N \to \pi N$	PWA GW-SAID WI08 (ED solution)	3,760
$\pi^- p \to \eta n$	$d\sigma/d\Omega$ (676), P (79)	755
$\pi^- p \to K^0 \Lambda$	$d\sigma/d\Omega$ (814), P (472), β (72)	1,358
$\pi^- p \to K^0 \Sigma^0$	$d\sigma/d\Omega$ (470), P (120)	590
$\pi^- p \to K^+ \Sigma^-$	$d\sigma/d\Omega$ (150)	150
$\pi^+ p \to K^+ \Sigma^+$	$d\sigma/d\Omega$ (1124), P (551) , β (7)	1,682
$\gamma p \to \pi^0 p$	$d\sigma/d\Omega$ (10743), Σ (2927), P (768), T (1404), $\Delta\sigma_{31}$ (140),	
	G (393), H (225), E (467), F (397), $C_{x'_L}$ (74), $C_{z'_L}$ (26)	17,564
$\gamma p \to \pi^+ n$	$d\sigma/d\Omega$ (5961), Σ (1456), P (265), T (718), $\Delta\sigma_{31}$ (231),	
	G (86), H (128), E (903)	9,748
$\gamma p \to \eta p$	$d\sigma/d\Omega$ (5680), Σ (403), P (7), T (144), F (144), E (129)	6,507
$\boldsymbol{\gamma p \to K^+ \Lambda}$	$d\sigma/d\Omega$ (2478), P (1612), Σ (459), T (383),	
	$C_{x'}$ (121), $C_{z'}$ (123), $O_{x'}$ (66), $O_{z'}$ (66), O_x (314), O_z (314),	5,936
	in total	**48,050**

Reaction	Observables (# data points)	p./channel
$\pi N \to \pi N$	PWA GW-SAID WI08 (ED solution)	3,760
$\pi^- p \to \eta n$	$d\sigma/d\Omega$ (676), P (79)	755
$\pi^- p \to K^0 \Lambda$	$d\sigma/d\Omega$ (814), P (472), β (72)	1,358
$\pi^- p \to K^0 \Sigma^0$	$d\sigma/d\Omega$ (470), P (120)	590
$\pi^- p \to K^+ \Sigma^-$	$d\sigma/d\Omega$ (150)	150
$\pi^+ p \to K^+ \Sigma^+$	$d\sigma/d\Omega$ (1124), P (551) , β (7)	1,682
$\gamma p \to \pi^0 p$	$d\sigma/d\Omega$ (10743), Σ (2927), P (768), T (1404), $\Delta\sigma_{31}$ (140),	
	G (393), H (225), E (467), F (397), $C_{x'_L}$ (74), $C_{z'_L}$ (26)	17,564
$\gamma p \to \pi^+ n$	$d\sigma/d\Omega$ (5961), Σ (1456), P (265), T (718), $\Delta\sigma_{31}$ (231),	
	G (86), H (128), E (903)	9,748
$\gamma p \to \eta p$	$d\sigma/d\Omega$ (5680), Σ (403), P (7), T (144), F (144), E (129)	6,507
$\boldsymbol{\gamma p \to K^+ \Lambda}$	$d\sigma/d\Omega$ (2478), P (1612), Σ (459), T (383),	
	$C_{x'}$ (121), $C_{z'}$ (123), $O_{x'}$ (66), $O_{z'}$ (66), O_x (314), O_z (314),	5,936
	in total	**48,050**

Data base

Reaction	Observables (# data points)	p./channel
$\pi N \to \pi N$	PWA GW-SAID WI08 (ED solution)	3,760
$\pi^- p \to \eta n$	$d\sigma/d\Omega$ (676), P (79)	755
$\pi^- p \to K^0\Lambda$	$d\sigma/d\Omega$ (814), P (472), β (72)	1,358
$\pi^- p \to K^0\Sigma^0$	$d\sigma/d\Omega$ (470), P (120)	590
$\pi^- p \to K^+\Sigma^-$	$d\sigma/d\Omega$ (150)	150
$\pi^+ p \to K^+\Sigma^+$	$d\sigma/d\Omega$ (1124), P (551) , β (7)	1,682
$\gamma p \to \pi^0 p$	$d\sigma/d\Omega$ (10743), Σ (2927), P (768), T (1404), $\Delta\sigma_{31}$ (140),	
	G (393), H (225), E (467), F (397), $C_{x'_L}$ (74), $C_{z'_L}$ (26)	17,564
$\gamma p \to \pi^+ n$	$d\sigma/d\Omega$ (5961), Σ (1456), P (265), T (718), $\Delta\sigma_{31}$ (231),	
	G (86), H (128), E (903)	9,748
$\gamma p \to \eta p$	$d\sigma/d\Omega$ (5680), Σ (403), P (7), T (144), F (144), E (129)	6,507
$\boldsymbol{\gamma p \to K^+\Lambda}$	$d\sigma/d\Omega$ (2478), P (1612), Σ (459), T (383),	
	$C_{x'}$ (121), $C_{z'}$ (123), $O_{x'}$ (66), $O_{z'}$ (66), O_x (314), O_z (314),	5,936
	[– beam-target obs. missing –]	
	in total	**48,050**

Fit result $K^+\Lambda$ photoproduction

EPJ A 54, 110 (2018)

simultaneous fit of $\gamma p \to \pi^0 p$, $\pi^+ n$, ηp, $K^+\Lambda$ and $\pi N \to \pi N$, ηN, $K\Lambda$, $K\Sigma$

$\gamma p \to K^+\Lambda$:

- Differential cross section

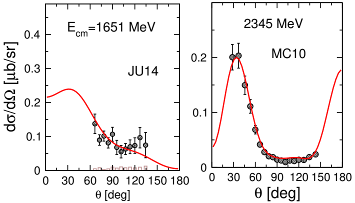

JU14: Jude PLB 735 (2014), MC10: McCracken PRC 81 (2010)

- Recoil polarization

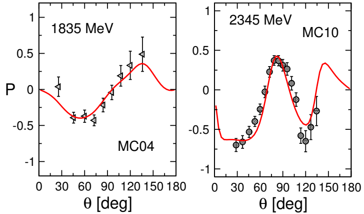

MC04: McNabb PRC 69 (2004), MC10: McCracken PRC 81 (2010)

- Beam asymmetry

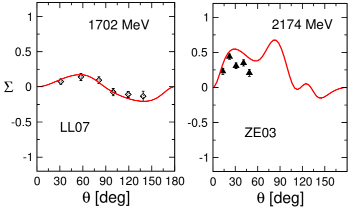

LL07: Lleres EPJA 31 (2007), ZE03: Zegers PRL (2003)

- Target asymmetry

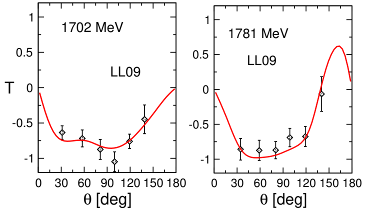

LL09: Lleres EPJA 39 (2009)

Fit result $K^+\Lambda$ photoproduction: beam-recoil asymmetries

EPJ A 54, 110 (2018)

simultaneous fit of $\gamma p \to \pi^0 p$, $\pi^+ n$, ηp, $K^+\Lambda$ and $\pi N \to \pi N$, ηN, $K\Lambda$, $K\Sigma$

$\gamma p \to K^+\Lambda$:

- $C_{x'}$

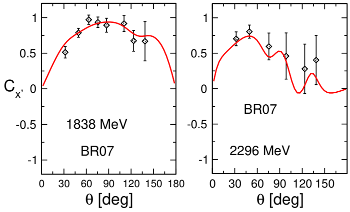

BR07: Bradford PRC 75 (2007)

- $C_{z'}$

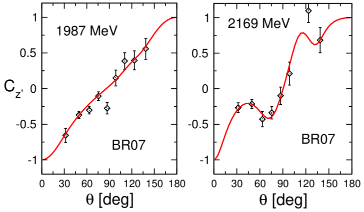

BR07: Bradford PRC 75 (2007)

- $O_{x'}$

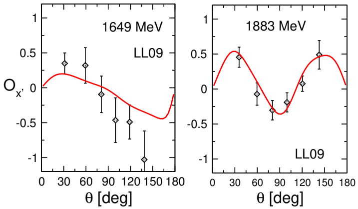

LL09: Lleres EPJA 39 (2009)

- $O_{z'}$

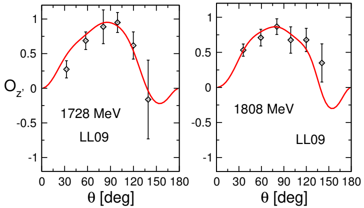

LL09: Lleres EPJA 39 (2009)

Fit result $K^+\Lambda$ photoproduction

EPJ A 54, 110 (2018)

simultaneous fit of $\gamma p \to \pi^0 p$, $\pi^+ n$, ηp, $K^+\Lambda$ and $\pi N \to \pi N$, ηN , $K\Lambda$, $K\Sigma$

- Fit of new CLAS data (Paterson *et al.* Phys. Rev. C 93, 065201 (2016)):

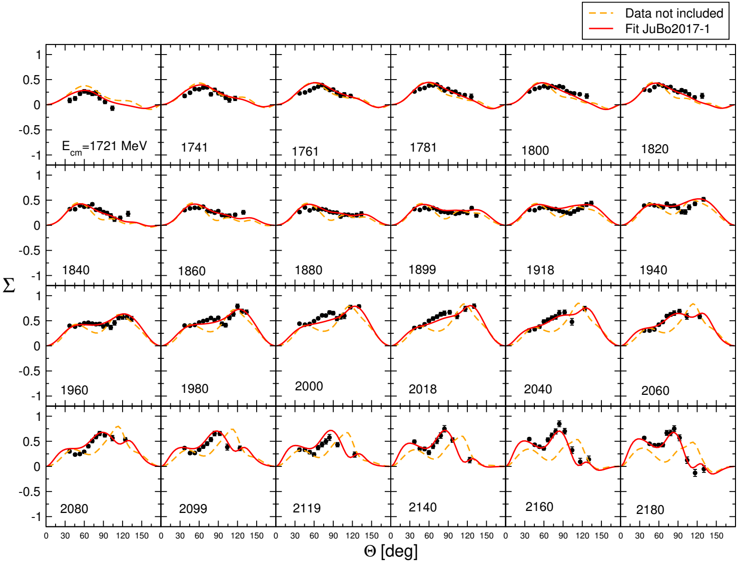

Fit result $K^+\Lambda$ photoproduction

EPJ A 54, 110 (2018)

simultaneous fit of $\gamma p \to \pi^0 p$, $\pi^+ n$, ηp, $K^+\Lambda$ and $\pi N \to \pi N$, ηN , $K\Lambda$, $K\Sigma$

- Fit of new CLAS data (Paterson *et al.* Phys. Rev. C 93, 065201 (2016)):

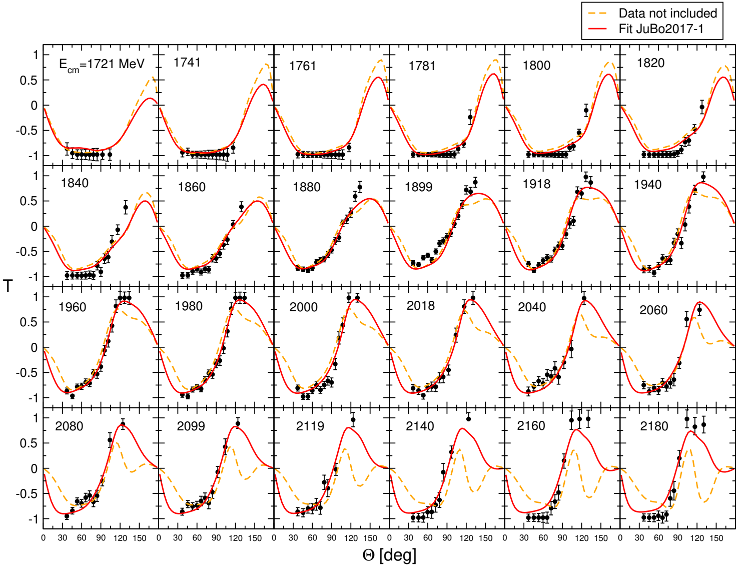

Fit result $K^+\Lambda$ photoproduction

simultaneous fit of $\gamma p \to \pi^0 p$, $\pi^+ n$, ηp, $K^+\Lambda$ and $\pi N \to \pi N$, ηN , $K\Lambda$, $K\Sigma$

- Fit of new CLAS data (Paterson *et al.* Phys. Rev. C 93, 065201 (2016)):

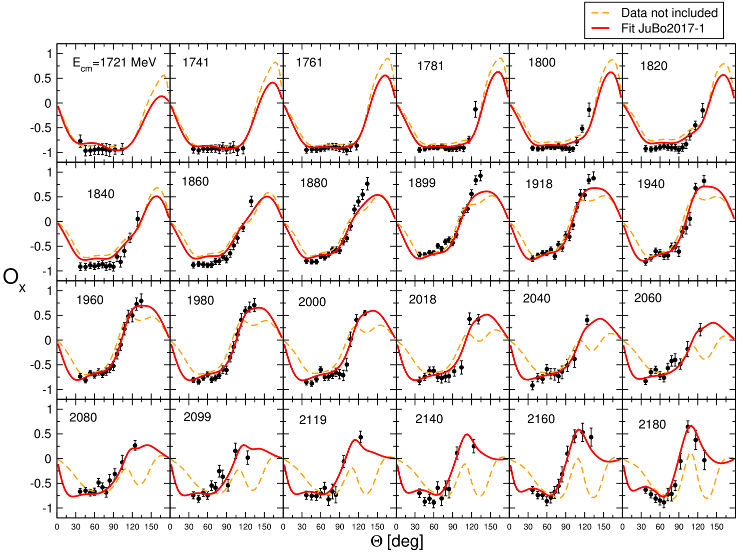

Fit result $K^+\Lambda$ photoproduction

simultaneous fit of $\gamma p \to \pi^0 p$, $\pi^+ n$, ηp, $K^+\Lambda$ and $\pi N \to \pi N$, ηN , $K\Lambda$, $K\Sigma$

- Fit of new CLAS data (Paterson *et al.* Phys. Rev. C 93, 065201 (2016)):

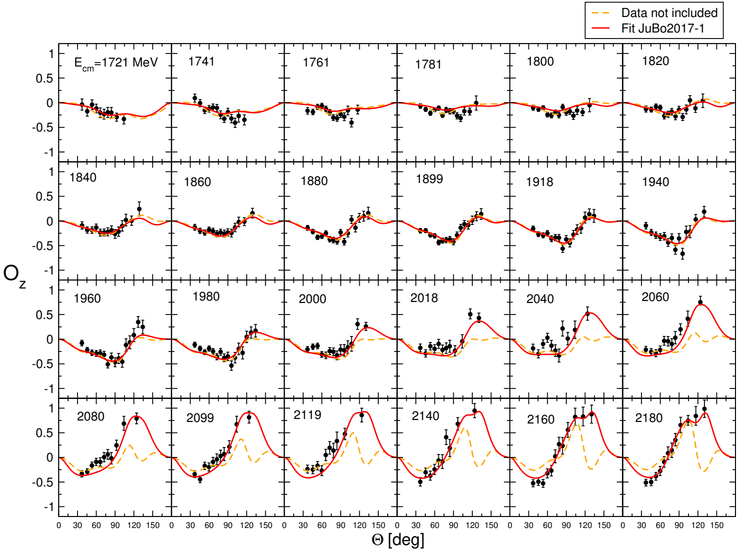

The resonance spectrum

Resonance spectrum

Resonance states: **Poles in the T-matrix** on the 2^{nd} Riemann sheet

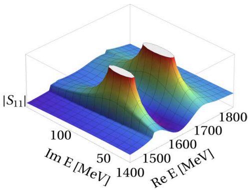

- $\mathrm{Re}(E_0)$ = "mass", $-2\mathrm{Im}(E_0)$ = "width"
- elastic πN residue $(|r_{\pi N}|, \theta_{\pi N\to\pi N})$, normalized residues for inelastic channels $(\sqrt{\Gamma_{\pi N}\Gamma_\mu}/\Gamma_{\mathrm{tot}}, \theta_{\pi N\to\mu})$
- photocouplings at the pole: $\tilde{A}^h_{pole} = A^h_{pole}\, e^{i\vartheta^h}$, $h = 1/2,\ 3/2$

$$\tilde{A}^h_{pole} = I_F \sqrt{\frac{q_p}{k_p}\,\frac{2\pi\,(2J+1)\mathbf{E_0}}{m_N\ \mathbf{r}_{\pi\mathrm{N}}}}\ \mathrm{Res}\, A^h_{L\pm}$$

I_F: isospin factor
q_p (k_p): meson (photon) momentum at the pole
$J = L \pm 1/2$ total angular momentum
E_0: pole position
$r_{\pi N}$: elastic πN residue
$A^h_{L\pm}$: helicity multipole

In the present analysis:

- all 4-star N and Δ states up to $J = 9/2$ are seen (exception: $N(1895)1/2^-$)
  + some states rated with less than 4 stars
- one additional s-channel diagram included: $N(1900)3/2^+$
- hints for new dynamically generated poles

Uncertainties of extracted resonance parameters

Challenges in determining resonance uncertainties, e.g.:

- **elastic πN channel**: not data but GWU SAID PWA

  $\rightarrow$ correlated χ^2 fit including the covariance matrix $\hat{\Sigma}$ (available on SAID webpage!) PRC 93, 065205 (2016)

  $$\chi^2(A) = \chi^2(\hat{A}) + (A - \hat{A})^T \hat{\Sigma}^{-1} (A - \hat{A})$$

  $A \sim$ vector of fitted PWs, $\hat{A} \sim$ vector of SAID SE PWs

  $\rightarrow$ same χ^2 as fitting to data up to nonlinear and normalization corrections

- **error propagation** data $\rightarrow$ fit parameters $\rightarrow$ derived quantities:
  bootstrap method: generate pseudo data around actual data, repeat fit

- **model selection**, significance of resonance signals:
  determine minimal resonance content using Bayesian evidence [PRL 108, 182002; PRC 86, 015212 (2012)]
  or the LASSO method [PRC 95, 015203 (2017); J. R. Stat. Soc. B 58, 267 (1996)]:

  $$\chi^2_T = \chi^2 + \lambda \sum_{i=1}^{i_{max}} |a_i|$$

  $\lambda \sim$ penalty factor, $a_i \sim$ fit parameter

  ↳ talk by R. Molina on Wednesday

Uncertainties of extracted resonance parameters

In JüBo framework: such methods are numerically challenging, but planned for the (near) future

Estimation of uncertainties of extracted resonance parameters in the present study:

- from 9 re-fits to re-weighted data sets
- individually increase the weight in each reaction channel
- extract resonance parameters from refits
- maximal deviation of resonance parameters of the refits = "error"
- only a qualitative estimation of relative uncertainties, absolute size not well determined

Resonance spectrum: selected results $I = 1/2,\ J^P = 3/2^+$

EPJ A 54, 110 (2018)

$N(1900)\ 3/2^+$ $****$	Re E_0 [MeV]	-2Im E_0 [MeV]	$\lvert r_{\pi N}\rvert$ [MeV]	$\theta_{\pi N\to\pi N}$ [deg]		
2017	1923(2)	217(23)	1.6(1.2)	−61(121)		
PDG 2018	1920 ± 20	150 ± 50	4 ± 2	−20 ± 30		
	$\frac{\Gamma^{1/2}_{\pi N}\Gamma^{1/2}_{\eta N}}{\Gamma_{tot}}$ [%]	$\theta_{\pi N\to\eta N}$	$\frac{\Gamma^{1/2}_{\pi N}\Gamma^{1/2}_{K\Lambda}}{\Gamma_{tot}}$ [%]	$\theta_{\pi N\to K\Lambda}$	$\frac{\Gamma^{1/2}_{\pi N}\Gamma^{1/2}_{K\Sigma}}{\Gamma_{tot}}$ [%]	$\theta_{\pi N\to K\Sigma}$
2017	1.1(0.7)	−10(79)	2.1(1.4)	1.7(86)	10(7)	−34(74)
PDG (BnGa)	5 ± 2	70 ± 60	3 ± 2	90 ± 40	4 ± 2	110 ± 30

$N(1720)\ 3/2^+$ $****$	Re E_0 [MeV]	-2Im E_0 [MeV]	$\lvert r_{\pi N}\rvert$ [MeV]	$\theta_{\pi N\to\pi N}$ [deg]		
2017	1689(4)	191(3)	2.3(1.5)	−57(22)		
2015-B	1710	219	4.2	−47		
PDG 2018	1675 ± 15	250^{+150}_{-100}	15^{+10}_{-5}	−130 ± 30		
	$\frac{\Gamma^{1/2}_{\pi N}\Gamma^{1/2}_{\eta N}}{\Gamma_{tot}}$ [%]	$\theta_{\pi N\to\eta N}$	$\frac{\Gamma^{1/2}_{\pi N}\Gamma^{1/2}_{K\Lambda}}{\Gamma_{tot}}$ [%]	$\theta_{\pi N\to K\Lambda}$	$\frac{\Gamma^{1/2}_{\pi N}\Gamma^{1/2}_{K\Sigma}}{\Gamma_{tot}}$ [%]	$\theta_{\pi N\to K\Sigma}$
2017	0.3(0.2)	139(35)	1.5(0.9)	−66(30)	0.6(0.4)	26(58)
2015-B	0.7	106	1.1	−70	0.2	79
PDG (BnGa)	3 ± 2	—	6 ± 4	−150 ± 45	—	—

Resonance spectrum: selected results $I = 1/2$, $J^P = 3/2^+$

$N(1900)\ 3/2^+$ $*\ *\ **$	Re E_0 [MeV]	-2Im E_0 [MeV]	$\lvert r_{\pi N}\rvert$ [MeV]	$\theta_{\pi N\to\pi N}$ [deg]		
2017	1923(2)	217(23)	1.6(1.2)	$-61(121)$		
PDG 2018	1920 ± 20	150 ± 50	4 ± 2	-20 ± 30		
	$\frac{\Gamma^{1/2}_{\pi N}\Gamma^{1/2}_{\eta N}}{\Gamma_{\text{tot}}}$ [%]	$\theta_{\pi N\to\eta N}$	$\frac{\Gamma^{1/2}_{\pi N}\Gamma^{1/2}_{K\Lambda}}{\Gamma_{\text{tot}}}$ [%]	$\theta_{\pi N\to K\Lambda}$	$\frac{\Gamma^{1/2}_{\pi N}\Gamma^{1/2}_{K\Sigma}}{\Gamma_{\text{tot}}}$ [%]	$\theta_{\pi N\to K\Sigma}$
2017	1.1(0.7)	$-10(79)$	2.1(1.4)	1.7(86)	10(7)	$-34(74)$
PDG (BnGa)	5 ± 2	70 ± 60	3 ± 2	90 ± 40	4 ± 2	110 ± 30

E_{1+}, M_{1+} multipoles in $\gamma p \to K^+\Lambda$:

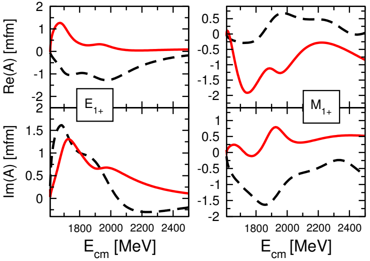

Red lines: JüBo2017

Black (dashed) lines: BnGa2014-02

Gutz *et al.* EPJ A 50, 74 (2014)

N(1900) $3/2^+$:

- seen by several other groups
- included ("by hand") to improve fit result for $\gamma p \to K^+\Lambda$

Resonance spectrum: selected results $I = 1/2$, $J^P = 3/2^+$

EPJ A 54, 110 (2018)

$N(1900)\ 3/2^+$ $****$	Re E_0 [MeV]	-2Im E_0 [MeV]	$\lvert r_{\pi N}\rvert$ [MeV]	$\theta_{\pi N\to\pi N}$ [deg]		
2017	1923(2)	217(23)	1.6(1.2)	$-61(121)$		
PDG 2018	1920 ± 20	150 ± 50	4 ± 2	-20 ± 30		
	$\frac{\Gamma^{1/2}_{\pi N}\Gamma^{1/2}_{\eta N}}{\Gamma_{\rm tot}}$ [%]	$\theta_{\pi N\to\eta N}$	$\frac{\Gamma^{1/2}_{\pi N}\Gamma^{1/2}_{K\Lambda}}{\Gamma_{\rm tot}}$ [%]	$\theta_{\pi N\to K\Lambda}$	$\frac{\Gamma^{1/2}_{\pi N}\Gamma^{1/2}_{K\Sigma}}{\Gamma_{\rm tot}}$ [%]	$\theta_{\pi N\to K\Sigma}$
2017	1.1(0.7)	$-10(79)$	2.1(1.4)	1.7(86)	10(7)	$-34(74)$
PDG (BnGa)	5 ± 2	70 ± 60	3 ± 2	90 ± 40	4 ± 2	110 ± 30

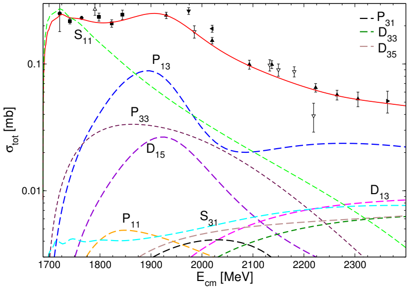

Total cross section $\pi^- p \to K^+\Sigma^-$

Resonance spectrum: selected results $I = 1/2$, $J^P = 5/2^-$

$N(1675)\ 5/2^-$ $****$	Re E_0 [MeV]	-2Im E_0 [MeV]	$\lvert r_{\pi N}\rvert$ [MeV]	$\theta_{\pi N\to\pi N}$ [deg]		
2017	1647(8)	135(9)	28(2)	$-22(3)$		
2015-B	1646	125	24	-22		
PDG 2018	1660 ± 5	135^{+15}_{-10}	28 ± 5	-25 ± 5		
	$\frac{\Gamma^{1/2}_{\pi N}\Gamma^{1/2}_{\eta N}}{\Gamma_{tot}}$ [%]	$\theta_{\pi N\to\eta N}$	$\frac{\Gamma^{1/2}_{\pi N}\Gamma^{1/2}_{K\Lambda}}{\Gamma_{tot}}$ [%]	$\theta_{\pi N\to K\Lambda}$	$\frac{\Gamma^{1/2}_{\pi N}\Gamma^{1/2}_{K\Sigma}}{\Gamma_{tot}}$ [%]	$\theta_{\pi N\to K\Sigma}$
2017	9.1(1.8)	$-45(3)$	0.7(0.2)	$-91(6)$	2.3(0.2)	$-175(10)$
2015-B	4.4	-43	0.1	100	3.1	-175
PDG 2018	—	—	—	—	—	—

dynamically generated

$N(2060)\ 5/2^-$ $***$	Re E_0 [MeV]	-2Im E_0 [MeV]	$\lvert r_{\pi N}\rvert$ [MeV]	$\theta_{\pi N\to\pi N}$ [deg]		
2017	1924(2)	201(3)	0.4(0.1)	172(12)		
PDG 2018	2070^{+60}_{-50}	400^{+30}_{-50}	20^{+10}_{-5}	-110 ± 20		
	$\frac{\Gamma^{1/2}_{\pi N}\Gamma^{1/2}_{\eta N}}{\Gamma_{tot}}$ [%]	$\theta_{\pi N\to\eta N}$	$\frac{\Gamma^{1/2}_{\pi N}\Gamma^{1/2}_{K\Lambda}}{\Gamma_{tot}}$ [%]	$\theta_{\pi N\to K\Lambda}$	$\frac{\Gamma^{1/2}_{\pi N}\Gamma^{1/2}_{K\Sigma}}{\Gamma_{tot}}$ [%]	$\theta_{\pi N\to K\Sigma}$
2017	0.2(0.2)	109(20)	2.2(0.2)	$-86(3)$	3.1(0.3)	86(3)
PDG (BnGa)	5 ± 3	40 ± 25	1 ± 0.5	—	4 ± 2	-70 ± 30

E_{2+}, M_{2+} multipoles in $\gamma p \to K^+\Lambda$:

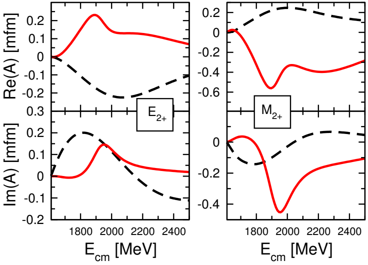

Red lines: JüBo2017

Black (dashed) lines: BnGa2014-02

Gutz *et al.* EPJ A 50, 74 (2014)

N(2060) $5/2^-$:

- seen by several other groups
- inconclusive indications already in previous JüBo fits (-2Im $E_0 > 600$ MeV)

dynamically generated

$N(2060)\ 5/2^-$ $***$	Re E_0 [MeV]	-2Im E_0 [MeV]	$\lvert r_{\pi N}\rvert$ [MeV]	$\theta_{\pi N\to\pi N}$ [deg]		
2017	1924(2)	201(3)	0.4(0.1)	172(12)		
PDG 2018	2070^{+60}_{-50}	400^{+30}_{-50}	20^{+10}_{-5}	-110 ± 20		
	$\frac{\Gamma^{1/2}_{\pi N}\Gamma^{1/2}_{\eta N}}{\Gamma_{\text{tot}}}$ [%]	$\theta_{\pi N\to\eta N}$	$\frac{\Gamma^{1/2}_{\pi N}\Gamma^{1/2}_{K\Lambda}}{\Gamma_{\text{tot}}}$ [%]	$\theta_{\pi N\to K\Lambda}$	$\frac{\Gamma^{1/2}_{\pi N}\Gamma^{1/2}_{K\Sigma}}{\Gamma_{\text{tot}}}$ [%]	$\theta_{\pi N\to K\Sigma}$
2017	0.2(0.2)	109(20)	2.2(0.2)	$-86(3)$	3.1(0.3)	86(3)
PDG (BnGa)	5 ± 3	40 ± 25	1 ± 0.5	—	4 ± 2	-70 ± 30

- $K\Lambda$ pure $I = 1/2$
- mixed isospin πN, $K\Sigma$ channels $\Rightarrow$ changes in $I = 3/2$ spectrum
- most of the well established Δ's similar to previous JüBo results
- in general larger uncertainties than for $I = 1/2$ ($\rightarrow$ extension to $\gamma N \rightarrow K\Sigma$!)

Example: $\Delta(1600)$ $3/2^+$

dynamically generated

$\Delta(1600)$ $3/2^+$ $****$	Re E_0 [MeV]	-2Im E_0 [MeV]	$\lvert r_{\pi N}\rvert$ [MeV]	$\theta_{\pi N\to\pi N}$ [deg]	$\frac{\Gamma^{1/2}_{\pi N}\Gamma^{1/2}_{K\Sigma}}{\Gamma_{tot}}$ [%]	$\theta_{\pi N\to K\Sigma}$ [deg]
2017	1579(17)	180(30)	11(6)	$-162(41)$	13(7)	$-21(40)$
2015-B	1552	350	23	-155	13	-5.6
PDG 2018	1510 ± 50	270 ± 70	25 ± 15	180 ± 30	—	—

	$A^{1/2}_{\text{pole}}$ $[10^{-3}\ \text{GeV}^{-\frac{1}{2}}]$	$\vartheta^{1/2}$ [deg]	$A^{3/2}_{\text{pole}}$ $[10^{-3}\ \text{GeV}^{-\frac{1}{2}}]$	$\vartheta^{3/2}$ [deg]
2017	54(25)	144(31)	46(19)	172(36)
2015-B	230	138	332	-71
BnGa [1]	53 ± 10	130 ± 15	55 ± 10	152 ± 15

[1] V. Sokhoyan *et al.* EPJ A51 95 (2015)

Summary and outlook

Impact of $K^+\Lambda$ photoproduction on the resonance spectrum in the JüBo DCC approach:

- confirmation of $N(1900)3/2^+$ and $N(2060)5/2^-$
- many resonances move closer to PDG values
- hints for additional new states

Outlook:

- extension to $K\Sigma$ photoproduction (already in progress)
- include πN covariance matrices in fit
- model selection methods (LASSO): find the minimal model, reduce number of fit parameters

Thank you for your attention!

Details of the formalism

Polynomials:

$$P_i^{\mathrm{P}}(E) = \sum_{j=1}^{n} g_{i,j}^{\mathrm{P}} \left(\frac{E - E_0}{m_N} \right)^j e^{-g_{i,n+1}^{P}(E-E_0)}$$

$$P_\mu^{\mathrm{NP}}(E) = \sum_{j=0}^{n} g_{\mu,j}^{\mathrm{NP}} \left(\frac{E - E_0}{m_N} \right)^j e^{-g_{\mu,n+1}^{\mathrm{NP}}(E-E_0)}$$

- $E_0 = 1077$ MeV
- $g_{i,j}^{\mathrm{P}}$, $g_{\mu,j}^{\mathrm{NP}}$: fit parameter
- $e^{-g(E-E_0)}$: appropriate high energy behavior
- $n = 3$

back

The scattering potential: s-channel resonances

$$V^{\mathrm{P}} = \sum_{i=0}^{n} \frac{\gamma^a_{\mu;i}\,\gamma^c_{\nu;i}}{z - m^b_i}$$

- i: resonance number per PW
- $\gamma^c_{\nu;i}$ ($\gamma^a_{\mu;i}$): creation (annihilation) vertex function with **bare coupling** f (free parameter)
- z: center-of-mass energy
- m^b_i: **bare mass** (free parameter)

- $J \leq 3/2$:

  $\gamma^c_{\nu;i}$ ($\gamma^a_{\mu;i}$) from effective $\mathcal{L}$

Vertex	$\mathcal{L}_{int}$
$N^*(S_{11})N\pi$	$\frac{f}{m_\pi}\bar{\Psi}_{N*}\gamma^\mu\vec{\tau}\,\partial_\mu\vec{\pi}\,\Psi \;+\;$ h.c.
$N^*(S_{11})N\eta$	$\frac{f}{m_\pi}\bar{\Psi}_{N*}\gamma^\mu\partial_\mu\eta\,\Psi \;+\;$ h.c.
$N^*(S_{11})N\rho$	$f\,\bar{\Psi}_{N*}\gamma^5\gamma^\mu\vec{\tau}\,\vec{\rho}_\mu\,\Psi \;+\;$ h.c.
$N^*(S_{11})\Delta\pi$	$\frac{f}{m_\pi}\bar{\Psi}_{N*}\gamma^5\vec{S}\partial_\mu\vec{\pi}\,\Delta^\mu \;+\;$ h.c.

- $5/2 \leq J \leq 9/2$:
  correct dependence on L (centrifugal barrier)

$$(\gamma^{a,c})_{\frac{5}{2}-} = \frac{k}{M}(\gamma^{a,c})_{\frac{3}{2}+} \qquad (\gamma^{a,c})_{\frac{5}{2}+} = \frac{k}{M}(\gamma^{a,c})_{\frac{3}{2}-}$$

$$(\gamma^{a,c})_{\frac{7}{2}-} = \frac{k^2}{M^2}(\gamma^{a,c})_{\frac{3}{2}-} \qquad (\gamma^{a,c})_{\frac{7}{2}+} = \frac{k^2}{M^2}(\gamma^{a,c})_{\frac{3}{2}+}$$

$$(\gamma^{a,c})_{\frac{9}{2}-} = \frac{k^3}{M^3}(\gamma^{a,c})_{\frac{3}{2}+} \qquad (\gamma^{a,c})_{\frac{9}{2}+} = \frac{k^3}{M^3}(\gamma^{a,c})_{\frac{3}{2}-}$$

The scattering potential: t- and u-channel exchanges

	πN	ρN	ηN	$\pi\Delta$	σN	$K\Lambda$	$K\Sigma$
πN	$N, \Delta, (\pi\pi)_\sigma$, $(\pi\pi)_\rho$	N, Δ, Ct., π, ω, a_1	N, a_0	N, Δ, ρ	N, π	Σ, Σ^*, K^*	Λ, Σ, Σ^*, K^*
ρN		N, Δ, Ct., ρ	-	N, π	-	-	-
ηN			N, f_0	-	-	K^*, Λ	Σ, Σ^*, K^*
$\pi\Delta$				N, Δ, ρ	π	-	-
σN					N, σ	-	-
$K\Lambda$						Ξ, Ξ^*, f_0, ω, ϕ	Ξ, Ξ^*, ρ
$K\Sigma$							Ξ, Ξ^*, f_0, ω, ϕ, ρ

Free parameters: cutoffs Λ in the form factors: $F(q) = \left(\frac{\Lambda^2 - m_x^2}{\Lambda^2 + \vec{q}^{\,2}}\right)^n$, $n = 1, 2$

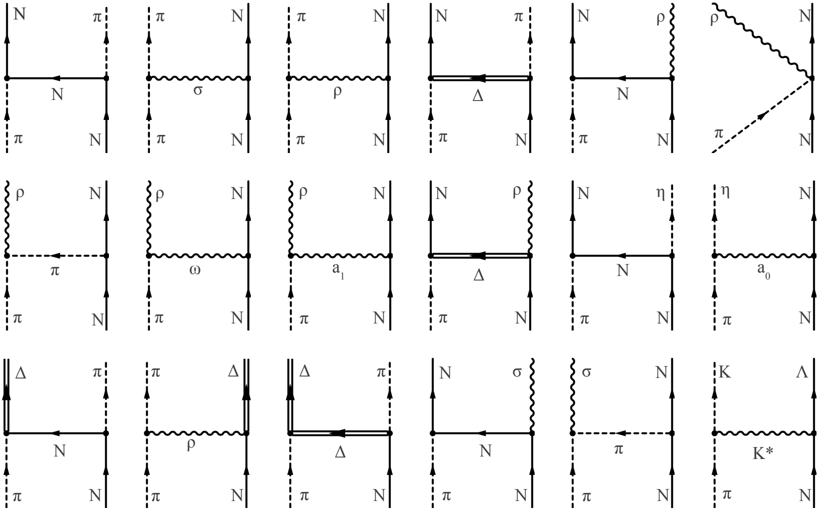
N π N π N
π N σ π N
π N ρ π N
N π Δ π N
N ρ N π N
ρ N π N
ρ N π π N
ρ N ω π N
ρ N a_1 π N
N ρ Δ π N
N η N π N
η N a_0 π N
Δ π N π N
π Δ ρ π N
Δ π Δ π N
N σ N π N
σ N π π N
K Λ K* π N

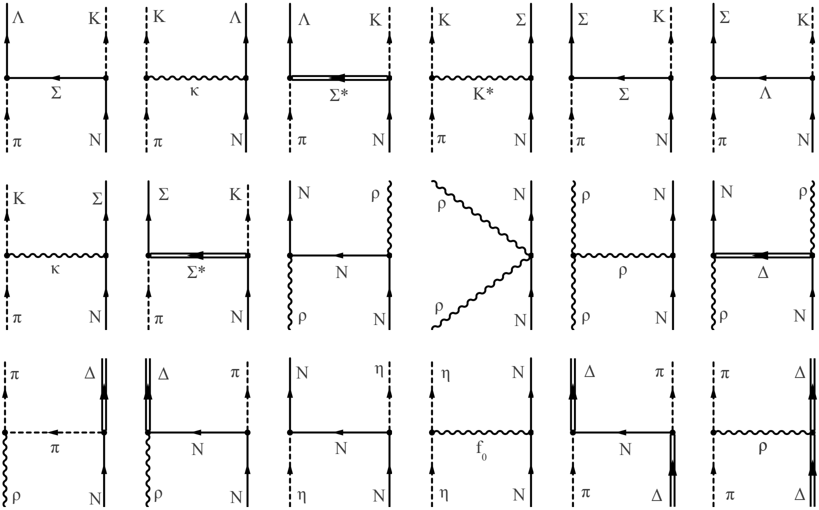

Λ K Σ π N
K Λ κ π N
Λ K Σ* π N
K Σ K* π N
Σ K Σ π N
Σ K Λ π N
K Σ κ π N
Σ K Σ* π N
N ρ N ρ N
ρ N ρ N
ρ N ρ ρ N
N ρ Δ ρ N
π Δ π ρ N
Δ π N ρ N
N η N η N
η N f0 η N
Δ π N π Δ
π Δ ρ π Δ

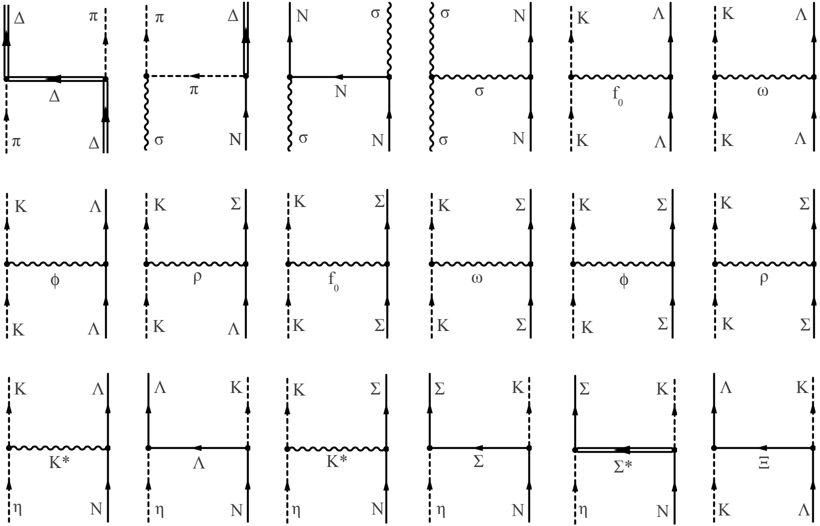
Δ π Δ π Δ
π Δ π σ N
N σ N σ N
σ N σ σ N
K Λ f_0 K Λ
K Λ ω K Λ
K Λ ϕ K Λ
K Σ ρ K Λ
K Σ f_0 K Σ
K Σ ω K Σ
K Σ ϕ K Σ
K Σ ρ K Σ
K Λ K* η N
Λ K Λ η N
K Σ K* η N
Σ K Σ η N
Σ K Σ* η N
Λ K Ξ K Λ

Interaction potential from effective Lagrangian

J. Wess and B. Zumino, Phys. Rev. **163**, 1727 (1967); U.-G. Meißner, Phys. Rept. **161**, 213 (1988); B. Borasoy and U.-G. Meißner, Int. J. Mod. Phys. A **11**, 5183 (1996).

- consistent with the approximate (broken) chiral $SU(2) \times SU(2)$ symmetry of QCD

Vertex	$\mathcal{L}_{int}$	Vertex	$\mathcal{L}_{int}$
$NN\pi$	$-\frac{g_{NN\pi}}{m_\pi}\Psi\gamma^5\gamma^\mu\vec{\tau}\cdot\partial_\mu\vec{\pi}\Psi$	$NN\omega$	$-g_{NN\omega}\bar{\Psi}[\gamma^\mu - \frac{\kappa_\omega}{2m_N}\sigma^{\mu\nu}\partial_\nu]\omega_\mu\Psi$
$N\Delta\pi$	$\frac{g_{N\Delta\pi}}{m_\pi}\bar{\Delta}^\mu\vec{S}^\dagger\cdot\partial_\mu\vec{\pi}\Psi$ + h.c.	$\omega\pi\rho$	$\frac{g_{\omega\pi\rho}}{m_\omega}\epsilon_{\alpha\beta\mu\nu}\partial^\alpha\vec{\rho}^\beta\cdot\partial^\mu\vec{\pi}\omega^\nu$
$\rho\pi\pi$	$-g_{\rho\pi\pi}(\vec{\pi}\times\partial_\mu\vec{\pi})\cdot\vec{\rho}^\mu$	$N\Delta\rho$	$-i\frac{g_{N\Delta\rho}}{m_\rho}\bar{\Delta}^\mu\gamma^5\gamma^\mu\vec{S}^\dagger\cdot\vec{\rho}_{\mu\nu}\Psi$ + h.c.
$NN\rho$	$-g_{NN\rho}\Psi[\gamma^\mu - \frac{\kappa_\rho}{2m_N}\sigma^{\mu\nu}\partial_\nu]\vec{\tau}\cdot\vec{\rho}_\mu\Psi$	$\rho\rho\rho$	$g_{NN\rho}(\vec{\rho}_\mu\times\vec{\rho}_\nu)\cdot\vec{\rho}^{\mu\nu}$
$NN\sigma$	$-g_{NN\sigma}\bar{\Psi}\Psi\sigma$	$NN\rho\rho$	$\frac{\kappa_\rho g^2_{NN\rho}}{2m_N}\bar{\Psi}\sigma^{\mu\nu}\vec{\tau}\Psi(\vec{\rho}_\mu\times\vec{\rho}_\nu)$
$\sigma\pi\pi$	$\frac{g_{\sigma\pi\pi}}{2m_\pi}\partial_\mu\vec{\pi}\cdot\partial^\mu\vec{\pi}\sigma$	$\Delta\Delta\pi$	$\frac{g_{\Delta\Delta\pi}}{m_\pi}\bar{\Delta}_\mu\gamma^5\gamma^\nu\vec{T}\Delta^\mu\partial_\nu\vec{\pi}$
$\sigma\sigma\sigma$	$-g_{\sigma\sigma\sigma}m_\sigma\sigma\sigma\sigma$	$\Delta\Delta\rho$	$-g_{\Delta\Delta\rho}\bar{\Delta}_\tau(\gamma^\mu - i\frac{\kappa_{\Delta\Delta\rho}}{2m_\Delta}\sigma^{\mu\nu}\partial_\nu)$
			$\cdot\vec{\rho}_\mu\cdot\vec{T}\Delta^\tau$
$NN\rho\pi$	$\frac{g_{NN\pi}}{m_\pi}2g_{NN\rho}\bar{\Psi}\gamma^5\gamma^\mu\vec{\tau}\Psi(\vec{\rho}_\mu\times\vec{\pi})$	$NN\eta$	$-\frac{g_{NN\eta}}{m_\pi}\bar{\Psi}\gamma^5\gamma^\mu\partial_\mu\eta\Psi$
NNa_1	$-\frac{g_{NN\pi}}{m_\pi}m_{a_1}\bar{\Psi}\gamma^5\gamma^\mu\vec{\tau}\Psi\vec{a}_\mu$	NNa_0	$g_{NNa_0}m_\pi\bar{\Psi}\vec{\tau}\Psi\vec{a}_0$
$a_1\pi\rho$	$-\frac{2g_{\pi a_1\rho}}{m_{a_1}}[\partial_\mu\vec{\pi}\times\vec{a}_\nu - \partial_\nu\vec{\pi}\times\vec{a}_\mu]\cdot[\partial^\mu\vec{\rho}^\nu - \partial^\nu\vec{\rho}^\mu]$	$\pi\eta a_0$	$g_{\pi\eta a_0}m_\pi\eta\vec{\pi}\cdot\vec{a}_0$
	$+\frac{2g_{\pi a_1\rho}}{2m_{a_1}}[\vec{\pi}\times(\partial_\mu\vec{\rho}_\nu - \partial_\nu\vec{\rho}_\mu)]\cdot[\partial^\mu\vec{a}^\nu - \partial^\nu\vec{a}^\mu]$		

Generalization to SU(3)

- t– and u–channel exchange: T^{NP}

  coupling constants fixed from SU(3) symmetry

  e.g. $g_{\Lambda NK} = -\frac{\sqrt{3}}{3} g_{NN\pi}(1 + 2\alpha_{BBP})$

  J. J. de Swart, Rev. Mod. Phys. **35**, 916 (1963) [Erratum-ibid. **37**, 326 (1965)].

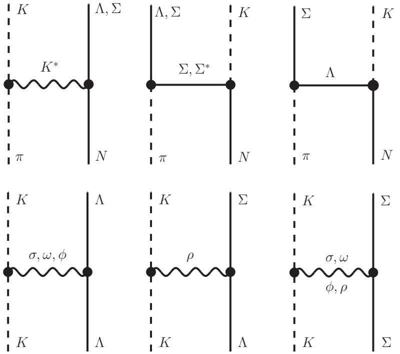

New free parameters: cutoffs Λ

- s-channel: resonances

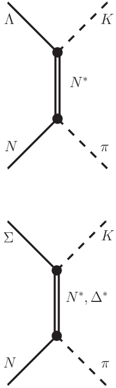

New free parameters:
bare couplings g_{N^*KY} and $g_{\Delta^*K\Sigma}$

Theoretical constraints of the S-matrix

Unitarity: probability conservation

- 2-body unitarity
- 3-body unitarity:

  discontinuities from t-channel exchanges

  $\rightarrow$ Meson exchange from requirements of the S-matrix [Aaron, Almado, Young, Phys. Rev. 174, 2022 (1968)]

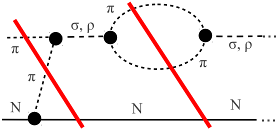

Analyticity: from unitarity and causality

- correct structure of branch point, right-hand cut (real, dispersive parts)
- to approximate left-hand cut $\rightarrow$ Baryon u-channel exchange

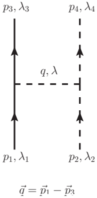

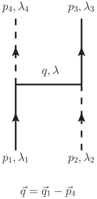

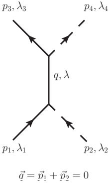

$\rightarrow$ Resonances

The SAID, BnGa and JüBo approaches

All three approaches:

- coupled channel effects
- unitarity (2 body)
- amplitudes are analytic functions of the invariant mass

SAID PWA

based on Chew-Mandelstam K-matrix

- K-matrix elements parameterized as energy-dependent polynomials
- resonance poles are dynamically generated (except for the $\Delta(1232)$)
- masses, width and hadronic couplings from fits to pion-induced πN and ηN production

Bonn-Gatchina (BnGa) PWA

Multi-channel PWA based on K-matrix (N/D)

- mostly phenomenological model
- resonances added by hand
- resonance parameters determined from large experimental data base:

  pion-, photon-induced reactions, 3-body final states

Jülich-Bonn (JüBo) DCC model

based on a Lippmann-Schwinger equation formulated in TOPT

- hadronic potential from effective Lagrangians
- photoproduction parameterized by energy-dependent polynomials
- resonances as s-channel states (dynamical generation possible)
- resonance parameters determined from pion- and photon-induced data

Construction of the multipole amplitude $M^{IJ}_{\mu\gamma}$

- **Field theoretical** approaches : DMT, ANL-Osaka, **Jülich-Athens-Washington**, ...

  Example: Gauge invariant formulation by Haberzettl, Huang and Nakayama

  Phys. Rev. C56 (1997), Phys. Rrev. C74 (2006), Phys. Rev. C85 (2012)

  - satisfies the generalized off-shell Ward-Takahashi identity
  - earlier version of the Jülich-Bonn model as FSI

Photoproduction amplitude:

$$M^\mu = \underbrace{M^\mu_s + M^\mu_u + M^\mu_t}_{\text{coupling to external legs}} + \underbrace{M^\mu_{int}}_{\text{coupling inside hadronic vertex}}$$

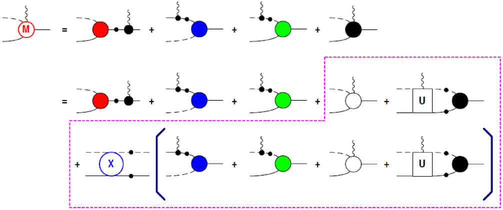

Strategy: Replace 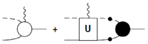

by phenomenological contact term such that the generalized WTI is satisfied

- Alternative gauge invariant chiral unitary method: Borasoy *et al.*, Eur. Phys. J. A **34** (2007) 161